JOURNAL OF MATERIALS SCIENCE 31 (1996) 4241–4247

Interface structure and reaction kinetics between SiC and thick cobalt foils

C. S. LIM, H. NICKEL, A. NAOUMIDIS*, E. GYARMATI
Institute for Materials in Energy Systems, Research Centre Jülich, D-52425 Jülich, Germany

Reaction couples of SiC with thick cobalt foils were annealed in an Ar–4 vol % H_2 atmosphere at temperatures between 950 and 1250 °C for times between 4 and 100 h. At temperatures above 950 °C, solid-state reactions lead to the formation of various silicides with carbon precipitates. The typical layer sequence in the reaction zone was determined by quantitative microanalysis to be SiC/CoSi + C/Co_2Si + C/Co_2Si/Co_2Si + C/ ... /Co_2Si/Co(Si)/Co. The mechanism of the periodic band structure formation with the carbon precipitation behaviour was discussed in terms of reaction kinetics and thermodynamic considerations. Two ternary phases, $CoSiC_2$ and Co_2SiC_3, unstable at room temperature, may exist in the system Co–Si–C. The growth of the reaction zone is dependent on the square root of time. The reaction kinetics are proposed to estimate the effective reaction constant from the parabolic growth of the reaction zone. The mechanical properties of the reaction zones were determined by the microhardness test.

1. Introduction

Solid-state reactions between ceramics and metals are of great interest in materials science because of the technological applications for devices fabricated with both ceramic and metal components. SiC is used for high-temperature applications in the form of a monolithic ceramic or in ceramic or metal–matrix composites [1–3]. SiC is also potentially a useful semiconducting material for high-temperature, high-frequency and high-power electronic devices [4–6]. In all these applications, as well as for the process of joining SiC and SiC to metal with metallic intermediates, detailed knowledge about SiC/metal interactions and the thermal stability of SiC/metal interfaces is of primary importance [7–9]. The chemical, thermal and crystallographic compatibility, which is dependent on the interfacial reaction, thermal expansion mismatch and lattice mismatch, must be considered to establish the thermal stress gradients across the reaction zone.

The properties of SiC–metal contacts are of increasing technological interest as the result of the large band gap of single-crystal SiC (2.9 eV) [5]. The large band gap allows SiC to be used in a variety of solid-state devices. In the case of other more common semiconducting devices, knowledge of the reactivity, thermal stability and electronic structure of semiconductor–metal interfaces is extremely important for understanding the devices and controlling device performances. One area of interest is the use of the low-temperature silicide-forming metals on SiC substrates in the attempt to form contacts after thermal annealing. Many metals have a strong tendency to interdiffuse at semiconductor/metal interfaces and most metals readily form carbides or silicides. A thorough characterization and understanding of SiC/metal interfaces, in terms of reactivity and thermal stability, is therefore crucial in the design of SiC devices.

Recently, a few studies of the interaction between SiC and various types of metals have been reported [10–15]. However, most work was phenomenological in nature because of the complex chemistry of interface formations, and the mechanisms proposed in the studies were somewhat obscure due to the complicated experimental conditions. In a previous study [15], the interfacial reaction and adhesion between SiC and thin sputtered cobalt films in the temperature range between 500 and 1450 °C were reported. The investigation aimed at providing the surface morphology, reaction products and adhesive strength using thin cobalt films deposited on SiC substrates. Because of the limited thickness of the thin cobalt films following exposure for a few hours at elevated temperature, the complete reaction path could not be determined in this investigation.

Therefore, more detailed information about the interfacial reaction is required for improved understanding of SiC/Co interfaces. In this work, we investigated the interface structure and reaction kinetics of SiC/Co from a different perspective, using thick metal foils. In more detail, the formed interface-like periodic band structure and carbon precipitation, were investigated. The mechanical properties of the reaction zones were examined by the microhardness test.

* Author to whom all correspondence should be addressed.
Please note C. S. Lim's present address is Department of Material Chemical Engineering, Chonnam National University, Kwangju 500-757, Korea

0022–2461

2. Experimental procedure

The materials used for the experiments were highly dense sintered α-SiC from "Elektroschmelzwerk Kempten", ESK, and thick cobalt foils from Alfa Prod./Johnson Matthey Company. The polycrystalline SiC contained 1.5 wt % total impurities, such as carbon and aluminium (ESK). The cobalt foil has a purity of 99.99% and a thickness of about 0.5–1 mm. SiC plates were cut into small pieces with a diameter of 20 mm and a thickness of 3 mm and ground with a BN/C disc. The SiC plates were then polished with a diamond disc using diamond pastes of 30, 15, 3, 1 μm and hyperliquids (polishing solution). The ceramic and metal samples were ultrasonically cleaned in ethanol, rinsed with water and dried. After polishing, the surface of SiC showed an average roughness of 4.7 nm measured by surface profilometry. As reported in a previous study [15], the surface SiC showed a typical mixed structure of globular to long/plate form, and the average grain size was about 4 μm.

Annealings were conducted in a high-temperature vacuum furnace with a graphite heating element manufactured by Degussa, Germany. The ceramic and metal reaction couples were placed in a graphite crucible and loaded with a weight of 5 kp (1 kp = 9.8067 N). The specimens were surrounded by titanium to remove the residual oxygen of the annealing time. After positioning the samples, the furnace was evacuated to 6×10^{-6} mbar (1 mbar = 10^2 Pa) and subsequently filled with a gas mixture of Ar/4 vol % H_2. The couples were annealed at temperatures between 950 and 1250 °C for 4–100 h. Thermocouples of type EL18(PtRh30/PtRh6) were used for the temperature measurement. The heating rate was set between 20 and 30 K min^{-1} and the cooling rate between 5 and 10 K min^{-1}.

The reaction couples were cut by a diamond disc and then embedded in copper resin. After mounting, the reaction couples were ground on a diamond disc, polished with diamond paste of 30, 15, 6, 3 and 1 μm and finished with an Al_2O_3 suspension. The polished cross-sections were investigated using optical microscopy and scanning electron microscopy (SEM). Quantitative atomic concentration profiles of silicon, carbon and cobalt were measured using electron probe microanalysis (EPMA). Mechanical properties of the reaction zone were determined with the microhardness test.

3. Results

3.1. Interface structure

Fig. 1 shows a cross-sectional view of the overall reaction zone of SiC/Co after annealing at 1050 °C for 64 h. The reaction zone consists of various kinds of distinct regions. This constitution could be identified by measurements using EPMA. Based on EPMA, qualitative analysis over the overall reaction zones is represented in the form of line scans for the elements silicon, carbon and cobalt in Fig. 2, which corresponds to the whole region in Fig. 1. Adjacent to the SiC, a grey layer was observed (Fig. 1b). Concentration

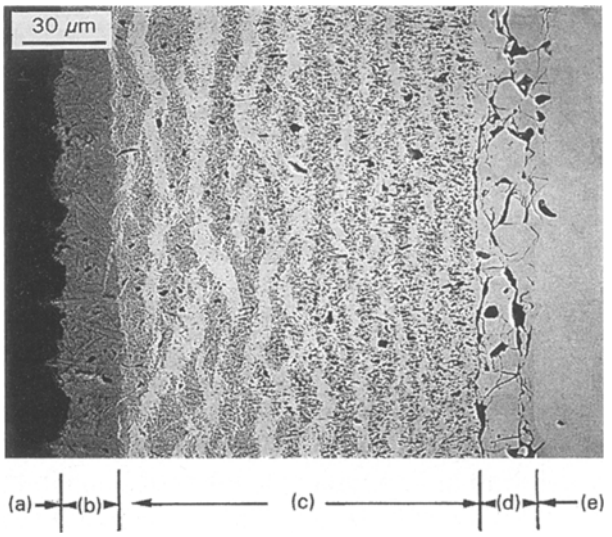

Figure 1 A cross-sectional view scanning electron micrograph of the overall reaction zone of SiC/Co after 64 h at 1050 °C; (a) SiC, (b) SiC reaction zone of CoSi + C, (c) alternating layers of Co_2Si + C/Co_2Si/Co_2Si + C/ ..., (d) metal reaction zone of Co_2Si and (e) cobalt metal.

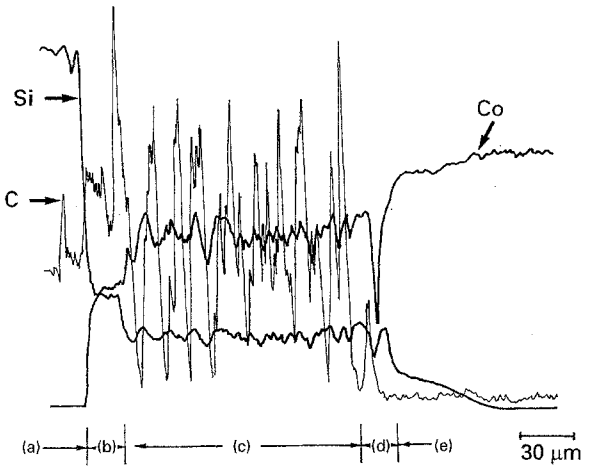

Figure 2 EPMA line scan for silicon, carbon and cobalt over the corresponding SiC/Co reaction zone in Fig. 1; (a) SiC, (b) SiC reaction zone of CoSi + C, (c) alternating layers of Co_2Si + C/Co_2Si/Co_2Si + C/ ..., (d) metal reaction zone of Co_2Si and (e) cobalt metal.

profiles across the SiC reaction zone, line-scanned by EPMA (Fig. 2b), indicate additional concentration for cobalt and a lower intensity for silicon compared to that in pure SiC phase. Adjacent to this reaction zone, a large reaction zone can be recognized with evidently higher cobalt and lower silicon content than that in the first mentioned reaction layer (Fig. 2c). The carbon intensity alternates in this region between zero and high maxima, corresponding to the bright and dark alternating layer sequences in Fig. 1c.

The microstructure of both reaction zones can be seen at a high magnification in Fig. 3a and b. The first SiC reaction zone is composed by much finer carbon precipitates in comparison to the zone further removed from the SiC reaction front. In this contact area the original microstructure of SiC can be recognized, where the precipitates are distributed texturally in a defined direction of the originally SiC crystal (Fig. 3a).

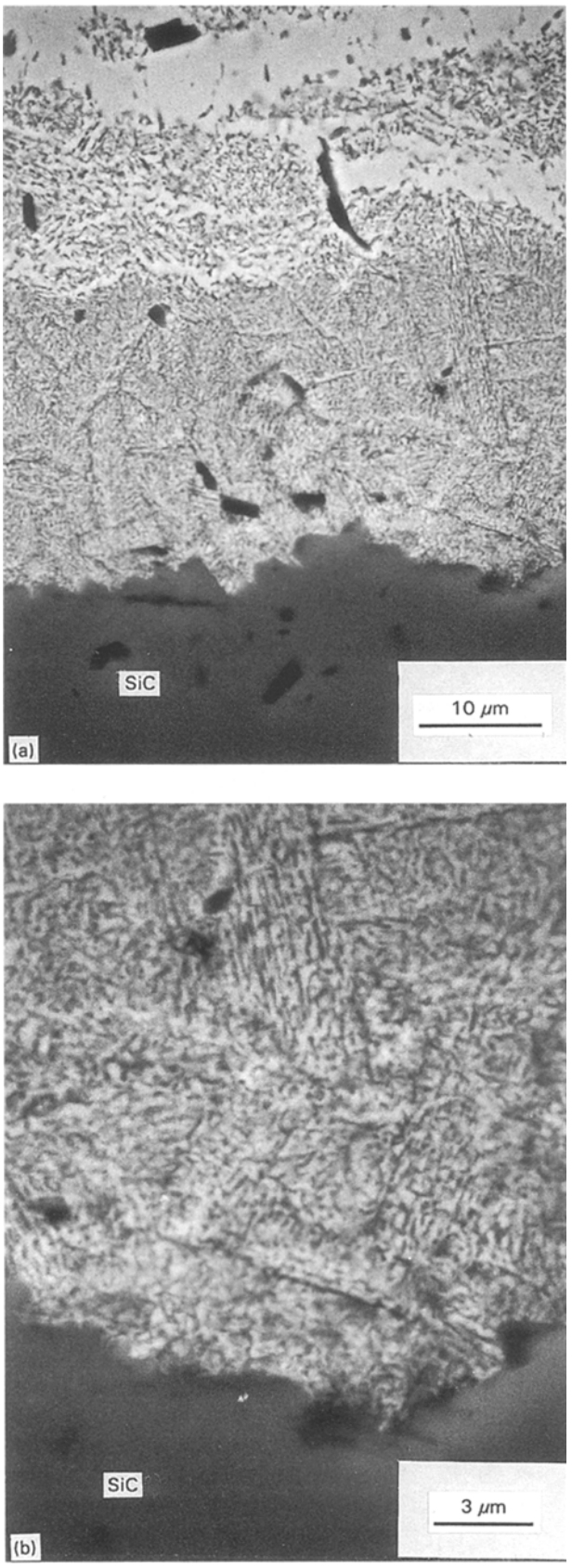

Figure 3 High-magnification scanning electron micrographs of the SiC reaction zone showing a relatively wide band of CoSi with fine carbon precipitates.

On the other hand, adjacent to the unreacted cobalt metal, a metallic similar reaction zone is formed with a large number of cracks (Fig. 1d) formed after the annealings in the examined temperature range between 950 and 1250 °C for various times. Characteristic of this zone is the absence of carbon precipitates. The line-scan of EPMA (Fig. 2d), also indicates the absence of carbon and a small intensity of silicon, which decreases continuously in the unreacted cobalt metal. According to this profile for silicon intensity, an inward diffusion of silicon into the cobalt metal was detected to a depth of 70 μm in Fig. 2e for this experiment.

Details of the carbon precipitates in the alternating layers are shown in the EPMA images of Fig. 4. The secondary electron image and X-ray maps with the distribution of the elements carbon, cobalt and silicon could be identified, so that the carbon is revealed to be in a regular arrangement in the reaction zone only in well-defined regions, where silicon and cobalt are more or less uniformly distributed in all the examined surfaces.

Integral quantitative analysis of the elements silicon, carbon and cobalt in all reaction zones was made with a defocused electron beam of the EPMA. The average concentrations are summarized in Table I. The analysis was performed over the corresponding SiC/Co reaction zone (Fig. 1) from the SiC over the SiC reaction zone with the various layers (first dark layer, second bright layer, third dark layer, ...) to the metallic phase and the unreacted cobalt. The average concentrations of cobalt and silicon in the first dark layer adjacent to SiC shows 25.7 wt % Si, 51.6 wt % Co and 23.5 wt % C corresponding to the values of 24.3 at % Si, 23.5 at % Co and 52.3 at % C. Assuming that the carbon is precipitated in a separated phase this atomic ratio indicates the presence of CoSi, while to two carbon atoms correspond to one CoSi. In the adjoining bright layer, the reaction phase of Co_2Si (with the concentrations of 20.6 wt % (32.0 at %) for silicon, 80.1 wt % (68.0 at %) for cobalt) is free of carbon. The concentration of carbon in all dark layers fluctuates between 21.5 and 23.5 wt %. It is noted that the amount of carbon does not increase or decrease systematically. The concentration relationship of Si/Co was also confirmed to be constant and independent of the presence of carbon. This atomic ratio corresponds to Co_2Si. The overall concentration of the three elements in the dark layers yields about three carbon atoms to one Co_2Si.

At a higher magnification, a scanning electron micrograph (Fig. 5) shows an easily distinguishable boundary between the bright layer from Co_2Si and the dark layer from $Co_2Si + 3C$ in detail. Some carbon particles are also partially and randomly distributed in the bright area. The dark area is featured by the fine carbon precipitation between Co_2Si phases. The composition of the cobalt silicide, Co_2Si, in the dark area is identical to that in the light area. The width of the bands of Co_2Si and $Co_2Si + 3C$ becomes smaller with increasing distance from the SiC reaction interface. Moreover, the periodic carbon precipitation is revealed by the structure change according to the location of the SiC reaction interface. This structure change of carbon could be observed through the reaction zone. It is due to the different thermodynamic driving force and kinetics between the reaction at the

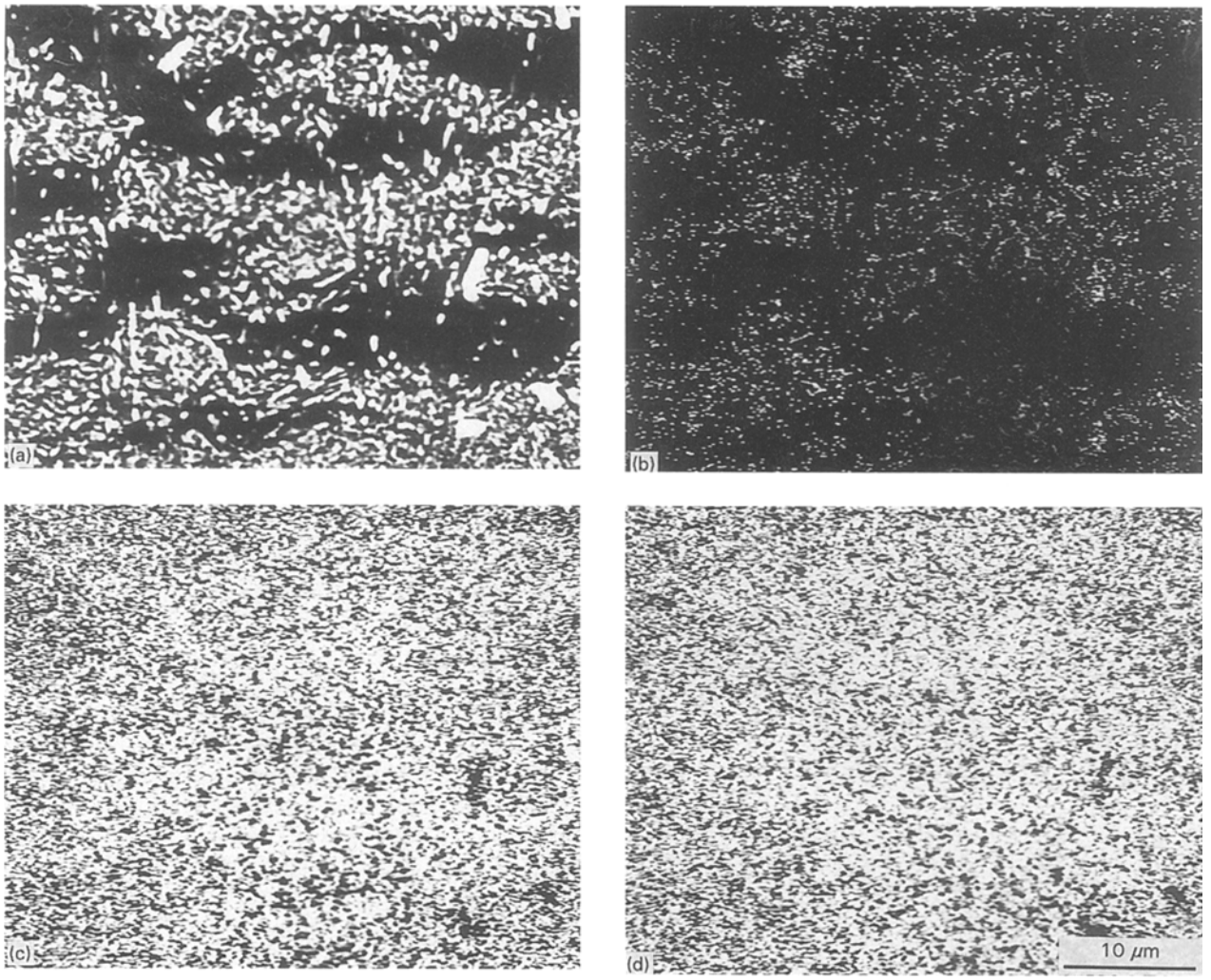

Figure 4 EPMA images of the alternating layers: (a) secondary electron image; (b) carbon X-ray map; (c) cobalt X-ray map; (d) silicon X-ray map.

TABLE I Average concentrations of silicon, cobalt and carbon in the SiC/Co reaction zone after 64 h at 1050 °C

Microstructure	Si (wt %)	Co (wt %)	C (wt %)
SiC	65.0	0.0	35.0
First dark layer	25.6	51.6	23.5
Second bright layer	20.6	80.1	0.0
Third dark layer	16.1	64.1	21.8
Fourth bright layer	20.7	80.4	0.0
Fifth dark layer	16.4	65.0	23.5
Sixth bright layer	20.6	79.9	0.0
Seventh dark layer	16.0	65.0	21.5
Eighth bright layer	20.5	79.8	0.0
Ninth dark layer	16.4	65.8	22.9
Tenth bright layer	20.6	80.2	0.0
Eleventh dark layer	16.2	65.8	22.5
Twelfth bright layer	20.6	80.3	0.0

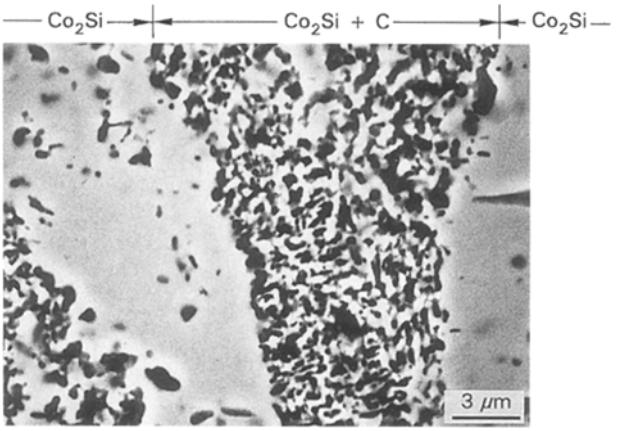

Figure 5 A scanning electron micrograph of the distinguishable boundary between Co_2Si and $Co_2Si + C$ phase in the alternating layer.

SiC reaction interface and the reaction at the metal reaction interface.

A scanning electron micrograph (Fig. 6) shows the metallic reaction zone in the area adjacent to cobalt. From quantitative analysis by EPMA, it was proved to be Co_2Si phase free of carbon precipitation. In contrast to the periodic band structure in this reaction zone, cracks and pores were observed for all SiC/Co samples. The thickness of this zone is about 25 μm after annealing at 1050 °C for 64 h.

3.2. Mechanical properties

The generation of cracks is caused by the various plastoelastic processes during cooling of the samples

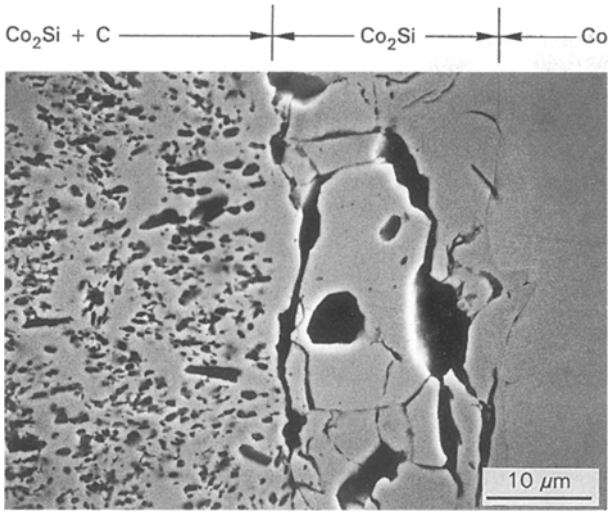

Figure 6 A scanning electron micrograph of the metal reaction zone.

TABLE II Average microhardness values in the SiC/Co reaction zone

Zone	Phase	Microhardness	
		($kp\,mm^{-2}$)	($10^3\,N\,mm^{-2}$)
Ceramic	SiC	3844	37.7
SiC reaction zone	CoSi + C	2691	26.39
CPZ[a]	Co_2Si + C	1267	12.43
CFZ[b]	Co_2Si	689	6.76
CPZ	Co_2Si + C	835	8.19
Metal reaction zone	Co_2Si	349	3.42
Metal	Co	232	2.28

[a] CPZ, Carbon precipitation zone.
[b] CFZ, Carbon-free zone.

from the annealing temperature, based on the various thermal expansion coefficients of the formed reaction phases. It has already been suggested [16, 17] that during the cooling process of a ceramic/metal reaction couple, critical tensile stress is induced at the ceramic edge and critical compressive stress at the metal edge. In the temperature ranges between 293 and 1273 K, the thermal expansion coefficients are $4.0–6.0 \times 10^{-6}$ K for SiC, $6.9–16.3 \times 10^{-6}$ K for cobalt and 11.1×10^{-6} K for CoSi. The SiC/Co reaction could be caused by the mismatch through the volume reduction of the reaction products. The formation of the reaction products Co_2Si + C and CoSi + C leads to a volume reduction of $\Delta V = -1.18$ and 0.74 $cm^3\,mol^{-1}$ SiC, respectively.

The mechanical properties of the total reaction zone were examined by the microhardness test. The average microhardness values of the different regions in the SiC/Co reaction zone are listed in Table II. The measurements were performed over the cross sections of this zone from the SiC and the SiC reaction layers to the metallic cobalt. The first reaction zone (CoSi + C) shows a substantially higher microhardness value of 2691 $kp\,mm^{-2}$, ($\sim 26.39 \times 10^3\,N\,mm^{-2}$), in comparison to the low value of 349 $kp\,mm^{-2}$ ($\sim 3.41 \times 10^3\,N\,mm^{-2}$) in the metal reaction zone. The value in the zone with the carbon precipitation

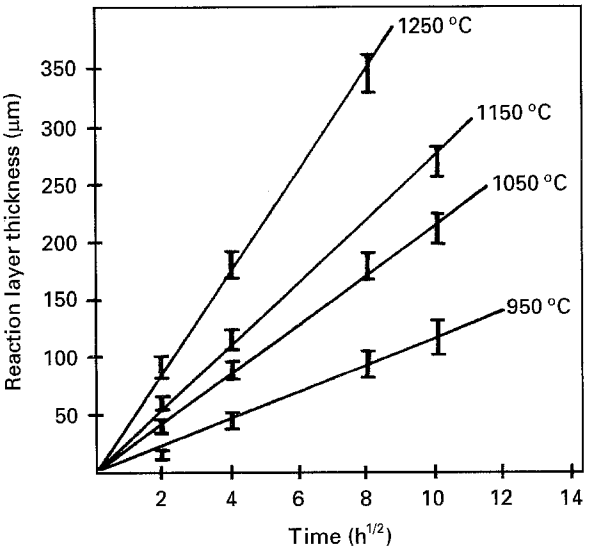

Figure 7 Growth of the reaction thickness in SiC/Co reaction zone versus square root of time for various times and temperatures.

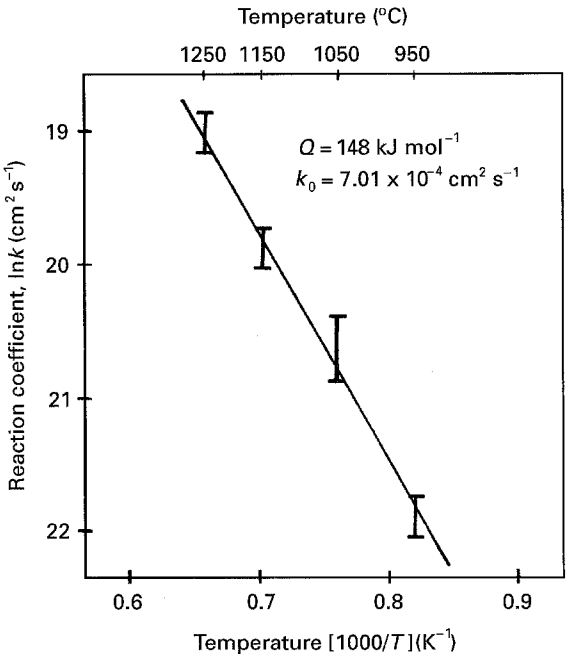

Figure 8 Reaction coefficients in SiC/Co reaction zone versus reciprocal absolute temperature [$\ln k = f(1/T)$].

(CPZ), Co_2Si + C, as well as in the carbon-free zone (CFZ) Co_2Si, decreases continuously from 1267 $kp\,mm^{-2}$ to 689 $kp\,mm^{-2}$ ($\sim 12.43 \times 10^3$ N mm^{-2} to $\sim 6.76 \times 10^3\,N\,mm^{-3}$). It is assumed that the value of the microhardness is a result of the microstructure and the internal stress in this area.

3.3. Reaction kinetics

The kinetics of the reaction SiC and Co were studied for temperatures betwen 950 and 1250 °C and times between 4 and 400 h. On the assumption that the reaction is diffusion-controlled, the thickness of the reaction zone follows a parabolic growth law. Therefore, the thicknesses of the reaction zone are plotted in Fig. 7 for various temperatures as a function of the

square root of annealing time. This relation shows a linear relationship indicating that the reaction is diffusion-controlled. The reaction coefficient, k, is equal to x^2/t and is dependent with the temperature according to the equation

$$k = k_0 \exp(-Q/RT) \quad (1)$$

where k_0 is the frequency factor and Q the activation energy of the chemical process. The relation of the logarithm of the reaction coefficients versus the reciprocal of the absolute temperature is linear, as plotted in Fig. 8. The activation energy and the frequency factor calculated from this relationship are 148 kJ mol^{-1} and 7.01×10^{-4} cm^2 s^{-1}, respectively. The activation energy is similar to the values for various metal silicides formed by reactions between silicon and metals at lower temperatures [18].

4. Discussion

The results will be discussed below in terms of interface structure and reaction kinetics, leading to the formation of cobalt silicides and carbon precipitates in the diffusion-controlled reaction zones. Considering the thermodynamics calculated by the Gibbs' free energy, ΔG, for various reactions, as given in the International Tables [19], the reaction products between SiC and Co could be correlated within this system. Table III shows Gibbs' free energy of the possible reactions at 1050 °C. The result predicts which phases are stable at the thermodynamic equilibrium. At temperatures of 1050 °C, cobalt is known to react with silicon to form three silicides CoSi, Co_2Si and $CoSi_2$, because the ΔG values for the formation of these compounds are negative. Less negative values are calculated for the corresponding reaction with SiC, i.e.

$$Co + SiC = CoSi + C \qquad \Delta G = -37.4 \text{ kJ mol}^{-1} \quad (2)$$

and

$$Co + 1/2SiC = 1/2Co_2Si + 1/2C$$
$$\Delta G = -33.5 \text{ kJ mol}^{-1} \quad (3)$$

because of the energy needed for SiC decomposition. The formation of $CoSi_2$ and Co_2C by the reaction with SiC is not thermodynamically possible at this temperature. The solid-state reaction between SiC and cobalt could generally be described as the formation of CoSi/C and Co_2Si/C, which results in the decomposition of SiC and the precipitation of carbon.

TABLE III Gibbs' free energy of possible reactions for SiC/Co system at 1050 °C

Possible reactions	Gibbs' free energy at 1050 °C (kJ mol^{-1})
$Co + 1/2SiC \Leftrightarrow 1/2Co_2C + 1/2Si$	27.5
$1\backslash 2Co + SiC \Leftrightarrow 1/2CoSi_2 + C$	2.4
$Co + SiC \Leftrightarrow CoSi + C$	− 37.4
$2Co + SiC \Leftrightarrow Co_2Si + C$	− 67.0
$1/2Co + Si \Leftrightarrow 1/2CoSi_2$	− 46.9
$Co + Si \Leftrightarrow CoSi$	− 86.7
$2Co + Si \Leftrightarrow Co_2Si$	− 99.6

These thermodynamic calculations are largely confirmed by the experimental results of this study. Moreover, the formation of layers with the following mixtures ranging from SiC to unreacted metallic cobalt was found:

1. CoSi + 2C;
2. Co_2Si;
3. Co_2Si + 3C;
4. Co_2Si with cracks; and finally
5. cobalt with dissolved silicon in graded concentration.

Layers 2 and 3 are repeated several times. The form of the carbon precipitates in the microstructure is indicative of the formation of this phase during the cooling process. In other words, prior to the formation of carbon precipitates, i.e. at the treatment temperature, a ternary phase of a cobalt carbosilicide with the composition $CoSiC_2$ was present in the first zone at the interfaces with SiC. In the layered zone between two Co_2Si films a carbosilicide with the formula Co_2SiC_3 was formed. The existence of ternary phases in the Co–Si–C system has not been reported in the literature to date. The formation of ternary phases in a metal–carbon–silicon phase diagram has already been mentioned on several occasions, for example in the Ti–C–Si system [20]. The Ti_2SiC_2 is a stable phase down to room temperature and was produced in pure form determining its physical properties [21, 22]. In the Co–C–Si system, this carbosilicide is not stable down to room temperature and is decomposed into Co_2Si and carbon, forming the dark layers observed on the cross-sections of the reacted samples. Moreover, this carbosilicide of cobalt apparently dissolves a rather large amount of Co_2Si in the temperature range examined. This solution has, then, a general composition of Co_2SiC_{3-x}. The solubility markedly decreases at lower temperatures and, finally, a phase separation into $Co_2Si + Co_2SiC_3$ takes place. In the experimental configuration examined, cooling in the furance is effected by heat radiation upon switching off the furnace. Under these conditions, the specimen surface was cooled first, and a certain temperature gradient was formed from the outside inwards. Under these conditions, different layers of the reaction zone formed reach the above temperature limits and lead to separation of the two phases, $Co_2Si + Co_2SiC_3$, at different times in the same way as observed in the microstructure of the reaction zone.

Future work with a high-temperature X-ray camera has to be done to establish this phase diagram at high temperatures and to determine the temperature limits of the reported transformations.

5. Conclusion

The solid-state reaction between SiC and thick cobalt foils at temperatures between 950 and 1250 °C for various times between 4 and 100 h leads to the formation of various silicides with carbon precipitations extending the periodic band structure of SiC/CoSi + C/Co_2Si + C/Co_2Si/ ... Co_2Si/Co in the reaction zone. The preferential reaction of

$Co + SiC = CoSi + C$ is exhibited at the SiC reaction interface, and the predominant reaction of $Si + 2Co = Co_2Si$ is present at the cobalt–metal reaction interface.

The thermodynamic driving force caused by the difference of the Gibbs' free energies for the possible reactions at the SiC interface and the cobalt interface causes a change of the interface structure with the carbon precipitation behaviour. The microanalysis of the periodic band structure formed in the SiC/Co reaction zone indicates the existence of ternary phases such as $CoSiC_2$, Co_2SiC_3, and Co_2SiC_{3-x} solid solutions at the temperature of the heat treatments. These ternary phases are unstable at the room temperatures and decompose in the binary phases CoSi, Co_2Si and carbon during the cooling process.

The generation of cracks is caused by the various plastoelastic processes and volume reduction of the reaction phases, SiC and metal. The average microhardness value has the tendency to decrease associated with the location of the SiC reaction interface. The reaction kinetics of growth in the thicknesses of the reaction zone shows a linear and parabolic relationship. The activation energy and the frequency factor are proposed to be $148\,kJ\,mol^{-1}$ and $7.01 \times 10^{-4}\,cm^2\,s^{-1}$.

References

1. K. D. MÖRGENTHALER, *Techn. Keram.* **1** (1988) 285.
2. L. M. SCHEPPARD, *Ceram. Bull.* **68** (1989) 1624.
3. D. L. McDANELS, T. T. SERAFINI and J. A. DICARLO, *J. Mater. Energy Systems* **8** (1986) 80.
4. G. L. HARRIS, M. G. SPENCER and C. Y. -W. YANG, "Amorphous and Crystalline Silicon Carbide III" (Springer, Berlin, Heidelberg, New York, 1992).
5. R. J. TREW, J. B. YAN and P. M. MOCK, *Proc. IEEE* **79** (1991) 598.
6. R. F. DAVIS, G. KELNER, M. SHUR, W. PALMOUR and J. A. EDMOND, *ibid.* **80** (1991) 677.
7. M. G. NICHOLAS, *Mater. Sci. Res.* **21** (1986) 349.
8. D. J. LARKIN, L. V. INTERRANTE and A. BOSE, *J. Mater. Res.* **5** (1990) 2706.
9. R. E. LOEHMAN, *Ceram. Bull.* **68** (1989) 891.
10. R. C. J. SCHIEPERS, F. J. J. VAN LOO and G. D. WITH, *J. Am. Ceram. Soc.* **71** (1988) C-284.
11. M. BACKHAUS-RICOULT, *Ber. Bunsenges. Phys. Chem.* **93** (1989) 1277.
12. T. C. CHOU, A. JOSHI and J. WADSWORTH, *J. Mater. Res.* **6** (1991) 796.
13. P. NIKOLOPOULOS, S. AGATHOPOULOS, G. N. ANGELOPOULOS, A. NAOUMIDIS and H. GRÜBMEIER, *J. Mater. Sci.* **27** (1992) 139.
14. E. GYARMATI, W. KESTERNICH and R. FÖRTHMANN, *cfi/Ber. DKG* **66** (1989) 292.
15. C. S. LIM, H. NICKEL, A. NAOUMIDIS and E. GYARTMATI, *J. Mater. Sci.* **30** (1995) 3874.
16. S. C. KUNZ and R. LOEHMAN, *Adv. Ceram. Mater.* **2** (1987) 69.
17. B. T. J. STOOP and G. den OUDEN, in "3rd International Conference on Joining Ceramics, Glass and Metal", edited by W. Kraft, DGM Inform. Ges. Verlag, Oberursel/D, Bad Nauheim (1989) p. 235.
18. S. S. LAU, J. W. MAYER, *J. Appl. Phys.* **49** (1978) 4005.
19. O. KUBASCHEWSKI and C. B. ALCOCK, "Metallurgical Thermochemistry" (Pergamon Press, Oxford, 1983) p. 280.
20. C. E. BURKL, "Ternary Phase Equilibria in Transition Metal–Boron–Carbon–Silicon Systems", Part II, Vol. III, AFML-TR-65-2 (US Air Force, 1965).
21. W. JEWITSCHKO and H. NOVOTNY, *M. Chem.* **98** (1967) 329.
22. E. GYARMATI, P. AHLADAS, A. NAOUMIDIS and H. NICKEL in "Proceedings of 13th International Plansee Seminar" Reutte/Tyrol, A, (1993), edited by H. Bildstein and R. Eck, *Metallwerk Plansee*, Reutte (1993) **2** p. 631.

Received 15 September 1995
and accepted 15 January 1996